Advantages of Combined Kinetic Analysis of Experimental Data Obtained under Any Heating Profile

L. A. Pérez-Maqueda,*,† J. M. Criado,† F. J. Gotor,† and J. Málek‡

Instituto de Ciencia de Materiales de Sevilla, C.S.I.C., Americo Vespucio s/n Isla de la Cartuja Sevilla 41010, Spain, and Joint Laboratory of Solid State Chemistry, Studentská 84, 532 10 Pardubice, Czech Republic

Received: June 14, 2001; In Final Form: November 5, 2001

The combined kinetic analysis of experimental data for solid-state reactions obtained under different experimental conditions is discussed. It is shown that the combined analysis of experimental data by means of the logarithmic expression of the general differential equation is a suitable method for the determination of the kinetic parameters. In the derivation of this equation, no assumptions are made of the way samples are heated. Therefore, any set of $T - \alpha - d\alpha/dt$ data should fit the equation regardless of the experimental procedure, i.e., isothermal, linear heating rate, modulated temperature, sample controlled, etc, used for their calculation. Thus, it can be used for the analysis of series of experiments performed under the same or different conditions. The method is tested with simulated and experimental curves obtained under different conditions. The kinetics of crystallization of $Ge_{0.3}Sb_{1.4}S_{2.7}$ glass is studied from a series of curves obtained under linear heating rate conditions. Additionally, the kinetics of decomposition of a siderite sample is also studied from a set of two curves obtained under linear heating and constant rate conditions.

1. Introduction

Experimental data for the kinetic analysis of solid-state reactions can be obtained under different experimental conditions. Thus, different temperature versus time programs have been proposed. In the traditional isothermal experiment, the sample is rapidly heated to a selected temperature and maintained at such temperature while the reaction evolution is recorded. Isothermal experiments are time-consuming, and for materials with low thermal conductivity, the steady-state cannot be reached until after the reaction has already started. To overcome such difficulties, the nonisothermal experiments have been proposed. Usually, in such experiments, temperature is increased under a linear heating rate program. Therefore, reaction evolution is recorded for a full range of temperatures.

Recently, new experimental methods where the sample behavior during heating determines the evolution of temperature versus time have been proposed.[1] Such methods are called sample-controlled thermal analysis (SCTA). One of the earliest and most extensively used examples of such experimental methods is the constant-rate thermal analysis (CRTA). The CRTA method implies the reaction temperature should be controlled in such a way that the reaction rate is maintained at a constant previously selected value. This method minimizes the influence of heat and mass-transfer phenomena. In addition, it has been used for the synthesis of materials with controlled texture and structure.[2−4] Another sample controlled thermal method very extensively used is the stepwise isothermal analysis.[5] In recent years, the main manufactures of thermal-analysis instruments have included the SCTA in their conventional equipment. Other experimental methods that has been recently proposed for the kinetic analysis of thermal solid-state reactions are the modulated TG[6] and the repeated temperature scanning thermal analysis.[7]

A number of procedures have been proposed in the literature for discriminating the kinetic model obeyed by the reaction from isothermal and nonisothermal data.[8−16] Recently,[17] some of the master-plots methods developed in the literature have been reexamined by using the concept of generalized time, θ, proposed by Ozawa.[14] It has been shown that the use of θ allows us to generalize the master plot curves and propose master plots that can be used simultaneously for any experimental data independently of the heating schedule used for obtaining the experimental results.

Although there is still a belief that kinetic parameters can be obtained from a single experiment, it has been pointed out in previous papers[18,19] that both the kinetic parameter and the kinetic model cannot be simultaneously obtained from a single experiment. Ozawa[20,21] has shown in recent papers that the "repeated temperature scanning" considerably improves both the discrimination of the reaction mechanism and the determination of the kinetic parameters from a single experiment because data equivalent to multiple isotherms, instead of a single one, can be obtained. However, this method does not allow us to perform the kinetic analysis of the whole reacted fraction range in every individual heating profile used along one of these experiments. This analysis is limited in every case to the narrow reaction range recorded at every particular cycle. This procedure perhaps would lead to wrong conclusions if, for instance, the forward reaction to be studied were influenced by heat and/or mass transfer phenomena. The combined kinetic analysis of a series of experimental traces independently recorded for the whole α range of the forward reaction under any heating schedule would report more complete kinetic information. This is the scope of the present work.

* To whom correspondence should be addressed.
† Instituto de Ciencia de Materiales de Sevilla.
‡ Joint Laboratory of Solid State Chemistry.

10.1021/jp012246b CCC: $22.00
Published on Web 03/05/2002

TABLE 1: Algebraic Expressions for the *f*(α) Functions for the Most Common Mechanisms in Solid-State Reactions

mechanism	symbol	*f*(α)
phase boundary controlled reaction (contracting area, i.e., bidimensional shape)	R2	$(1-\alpha)^{1/2}$
phase boundary controlled reaction (contracting volume, i.e., tridimensional shape)	R3	$(1-\alpha)^{2/3}$
unimolecular decay law (instantaneous nucleation and unidimensional growth)	F1	$(1-\alpha)$
random nucleation and growth of nuclei (Avrami−Erofeev equation)[a]	Am	$m(1-\alpha)[-\ln(1-\alpha)]^{1-1/m}$
two-dimensional diffusion (bidimensional particle shape)	D2	$1/[-\ln(1-\alpha)]$
three-dimensional diffusion (tridimensional particle shape) Jander equation	D3	$3(1-\alpha)^{2/3}/2[1-(1-\alpha)^{1/3}]$
three-dimensional diffusion (tridimensional particle shape) Ginstein−Brounshtein equation	D4	$3/2[(1-\alpha)^{-1/3}-1]$

[a] This formal kinetic law generally applies for random nucleation and growth of nuclei, although they are two different processes with different kinetic parameters. The nuclei are very often formed during the induction period. In such a case, the α−*t* (or *T*) plots would represent the growth process from preexisting nuclei and the experimental data would be fitted with a single set of kinetic parameters (*E* and *A*).

2. Theoretical

For a solid-state reaction that is ruled by a single process, the reaction rate can be expressed by means of the general law

$$\frac{d\alpha}{dt} = A\exp(-E/RT)f(\alpha) \tag{1}$$

with α being the reacted fraction at time *t*, *A* being the preexponential factor of Arrhenius, *T* being the absolute temperature, and *f*(α) is a function depending on the reaction mechanism. Table 1 includes the function for the most commonly used mechanisms in solid-state reactions.

The logarithmic form of the general kinetic equation (eq 1) after rearranging terms can be written as follows:

$$\ln\left(\frac{d\alpha/dt}{f(\alpha)}\right) = \ln A - E/RT \tag{2}$$

This latter equation is well-known[8] for calculating the kinetic parameters,where *E* is obtained from the slope of the line obtained from the plot of the left-hand side of eq 2 versus the reciprocal of temperature. The preexponential factor is obtained from the intercept of such plot. The universality of this equation is supported by Ozawa who has previously stated that the isoconversional Friedman−Ozawa plot (based on eq 2) can be applied to data obtained by all mode of temperature change.[7,20]

It was shown in a previous paper[17] that the reduced time concept introduced by Ozawa[14] allows us to propose generalized master plots that can be applied whatever the heating schedule used for recording the experimental data. The kinetic rate equation at infinite temperature is obtained from the generalized time defined as[14]

$$\theta = \int_0^t \exp\left(\frac{-E}{RT}\right) dt \tag{3}$$

where θ denotes the reaction time taken to attain a particular α at infinite temperature. Differentiation of eq 3 leads to[22,23]

$$\frac{d\theta}{>dt} = \exp\left(\frac{-E}{RT}\right) \tag{4}$$

When eqs 1 and 4 are combined, the following expression is obtained:

$$\frac{d\alpha}{d\theta} = Af(\alpha) \tag{5}$$

or

$$\frac{d\alpha}{d\theta} = \frac{d\alpha}{dt}\exp\left(\frac{E}{RT}\right) \tag{6}$$

where $d\alpha/d\theta$ corresponds to the generalized reaction rate, obtained by extrapolating the reaction rate in real time, $d\alpha/dt$, to infinite temperature.

Using the reference point at $\alpha = 0.5$, the following equation is easily derived from eq 5:

$$\frac{d\alpha/d\theta}{(d\alpha/d\theta)_{0.5}} = \frac{f(\alpha)}{f(0.5)} \tag{7}$$

where *f*(0.5) is a constant for a given kinetic model function. Equation 7 indicates that, at a given α, the experimental value of the reduced-generalized reaction rate, $(d\alpha/d\theta)/(d\alpha/d\theta)_{\alpha=0.5}$, and theoretically calculated value of $f(\alpha)/f(0.5)$ are equivalent when an appropriate *f*(α) for describing the rate process under investigation is applied. Because both the values depend only on α, comparison of the experimental plot of $(d\alpha/d\theta)/(d\alpha/d\theta)_{\alpha=0.5}$ against α with the theoretical plots of $f(\alpha)/f(0.5)$ against α, drawn by assuming various *f*(α) functions, is methodologically identical to the conventional master plot method. The master plots resulting from the different kinetic model included in Table 1 were included in a previous work.[17] According to eq 5, the reduced reaction rate has the following relationship to the experimental kinetic data:

$$\frac{d\alpha/d\theta}{(d\alpha/d\theta)_{\alpha=0.5}} = \frac{d\alpha/dt}{(d\alpha/dt)_{\alpha=0.5}}\frac{\exp(E/RT)}{\exp(E/RT)} \tag{8}$$

where $T_{0.5}$ is the reaction remperature at $\alpha = 0.5$.

In order to calculate the experimental value of $(d\alpha/d\theta)/(d\alpha/d\theta)_{\alpha=0.5}$, the temperature conditions of the experimental kinetic data have to be taken into account. For the experimental kinetic

data under isothermal conditions, both the exponential term in eq 8 offset each other because $T = T_{0.5}$, so that the experimental master plot can be derived directly from a single isothermal curve of $d\alpha/dt$ against α. On the other hand, for all nonisothermal data, the exponential term in eq 8 cannot be canceled out. In order to calculate the reduced reaction rate at a given α from nonisothermal data under linear and nonlinear heating, in addition to the kinetic data of a single measurement, the value of E for the process should be known previously. As a special case for the nonlinear nonisothermal data, the ratio of rate terms in real time in eq 8 is to be unity for the kinetic data of CRTA.

The comparison of the values of $(d\alpha/d\theta)/(d\alpha/d\theta)_{\alpha=0.5}$ determined from the experimental data by means of eq 8 with the master plots determined from eq 7 for the different kinetic model proposed in the literature for describing solid-state reactions will be used for testing the kinetic model.

3. Materials and Methods

A sample of $Ge_{0.3}Sb_{1.4}S_{2.7}$ glass was prepared in a evacuated silica ampule from pure elements (99.999% purity), by melting and homogenization at 950 °C for 12 h. Siderite sample ($FeCO_3$) was a natural mineral from Cala (Spain). Its chemical analysis by X-ray fluorescence spectrometry is Fe_2O_3, 44.6%; MgO, 10.8%; Mn_2O_3, 3.7%; CaO, 1.1%; SiO_2, 4.9%; others, 0.9%; ignition loss, 34.0%.

The X-ray diffraction (XRD) analysis of this sample shows the presence of small amounts of calcite, dolomite, and quartz. The unit cell parameters refined from the XRD pattern are $a = 4.6739$ and $c = 15.246$. These parameters are consistent with a nominal composition of $\sim(Fe_{0.7}Mg_{0.3})CO_3$ according to previous results.[24]

Differential scanning calorimetric (DSC) measurements were performed (model DSC-7, Perkin-Elmer) on ~10 mg bulk samples encapsulated in standard aluminum sample pans, in an atmosphere of dry nitrogen. The instrument was calibrated with indium, lead, and zinc standards. Experiments were performed under linear heating rate conditions.

The thermogravimetric (TG) measurement under a linear heating rate condition was carried out with a electrobalance (model 2000, Cahn) connected to a conventional high vacuum system equipped with a Penning gauge. Small amounts of the sample (~14 mg) and heating rates (0.52 K min^{-1}) were used to minimize the heat and mass transfer phenomena. Thus, the total pressure above the sample never exceed 10^{-4} mbar.

Constant rate thermal analysis (CRTA) was performed in the same instrument, but the temperature was controlled in such a way that the decomposition rate was maintained constant during the entire experiment. This was achieved by interfacing the output of the Penning gauge to the furnace controller; thus, the pressure was maintained as a constant at a previously selected value inside the instrument during the decomposition reaction. A similar setup was proposed by Rouquerol.[1,25]

4. Results

4.1. Check of the Method from Theoretical Curves. Figure 1 shows a theoretical simulated curve drawn by assuming linear heating rate conditions (heating rate, β, 10 K min^{-1}), a F1 kinetic model, and the following kinetic parameters: $E = 167$ kJ mol^{-1} and $A = 9.6\ 10^7$ min^{-1}. This curve has been calculated from the numerical integration of eq 1 using the Runge−Kutta procedure included in the Mathcad software[26] with an error in the calculation lower than 10^{-5}%. The simulated curve was analyzed by means of the conventional differential kinetic analysis method after considering the $f(\alpha)$ functions proposed in the literature for describing solid-state reactions as shown in Table 1. The analysis was performed in the range of $0.2 \leq \alpha \leq 0.8$. This range has been selected because, although theoretical curves are free of error, experimental curves have experimental error mainly for low and high values of α, and therefore, kinetic studies are very often limited to such a range. Table 2 includes the resulting activation energies, the Arrhenius preexponential factors, and the Pearson's r correlation coefficient for the kinetic models included in Table 1. It can be observed that very good correlation coefficients are obtained for most of the kinetic models considered, which points out that it is not possible to obtain the kinetic parameters and discriminating the kinetic model from a single TG or DTG curve.[18,19] This conclusion is confirmed by the results included in Figure 1 that show that the TG and DTG traces calculated for A2 and A3 kinetic models with the apparent values of E and A included in Table 2 fit the curves simulated for a F1 kinetic model.

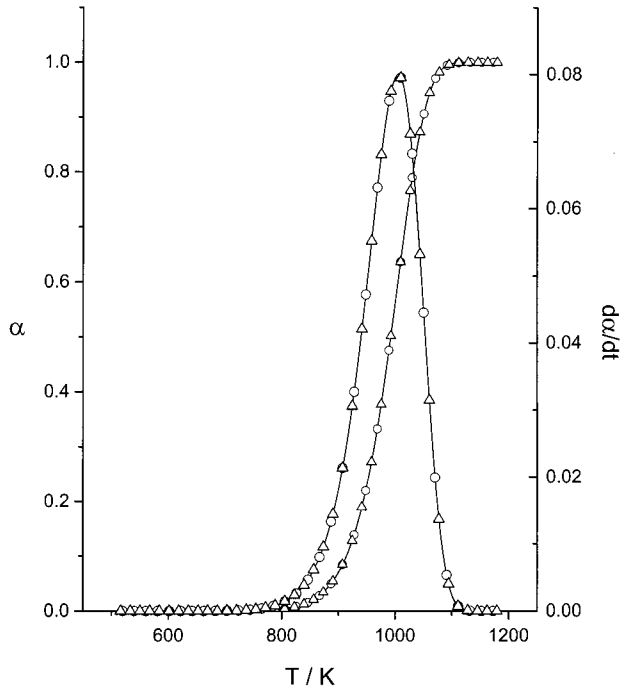

Figure 1. Simulated curves by assuming linear heating rate conditions (heating rate, β, 10 K min^{-1}), an F1 kinetic model, and the following kinetic parameters: $E = 167$ kJ mol^{-1} and $A = 9.6\ 10^7$ min^{-1} (solid line). Fitting of these curves by A2 (○) and A3 (△) kinetic models with the corresponding kinetic parameters included in Table 2.

TABLE 2: Kinetic Parameters Obtained from the Kinetic Analysis of the Curve Illustrated in Figure 1 by Assuming Different Kinetic Models

kinetic model	E (KJ mol^{-1})	A (min^{-1})	r
F1	167.0	9.6×10^7	1
R2	107.8	4.6×10^4	0.98
R3	88.1	3.6×10^3	0.95
A1.5	106.0	4.5×10^4	1
A2	75.6	8.9×10^2	1
A3	45.1	15.8	1
D2	231.2	6.4×10^{10}	0.98
D3	291.3	3.3×10^{13}	0.997
D4	251.9	2.1×10^{11}	0.99

For a set of rising temperature experiments obtained at different heating rates, only one kinetic model fits simultaneously all of the data. Figure 2 shows a set of curves simulated by assuming different linear heating rates, $\beta = 2$, 5, 10, and 15, and the same kinetic parameters as those used in the simulation of the F1 curves included in Figure 1. The differential

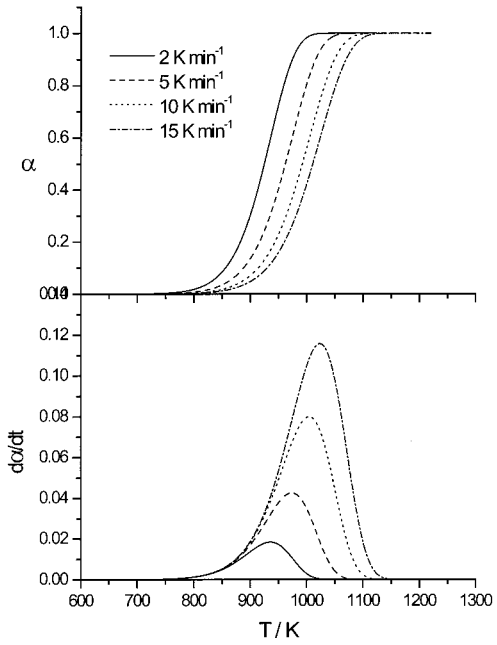

Figure 2. Simulated curves by assuming different heating rates (β = 2, 5, 10, and 15 K min^{-1}, respectively), a F1 kinetic model, and the following kinetic parameters: E = 167 kJ mol^{-1} and A = 9.6 10^7 min^{-1}.

method described in the Experimental Section was originally proposed for analyzing a single curve obtained under linear heating rate conditions, where the method is derived directly from the general eq 1 and no assumptions are made on the way the sample is heated. Therefore, it can be applied simultaneously to data obtained under any different heating rates. The four curves obtained under different heating rate conditions (illustrated in Figure 2) are analyzed at the same time by the differential method in Figure 3. This figure shows that only when the correct kinetic model is assumed all of the experimental points lie on a single straight line whose slope and intercept gives respectively the same values of the activation energy and the preexponential factor of Arrhenius as those used for the simulation. On the other hand, when any kinetic model other than the one assumed for simulating the DTG curves is considered, the calculated data are spread in different lines being quite clear that the data cannot be fitted at all by a unique straight line.

As it was stated before, eq 2 should fit any data obtained under any experimental conditions; therefore, experimental curves obtained by different techniques could be analyzed at the same time by eq 2. A set of three curves (Figure 4) have been simulated assuming in all cases an A2 kinetic model and the following kinetic parameters: $A = 10^5$ min^{-1}, E = 100 kJ mol^{-1}. One curve is simulated assuming linear heating rate conditions (β = 10 K min^{-1}), another curve is constructed under isothermal conditions at T = 900 K and, finally, the last curve is simulated under constant reaction-rate conditions (CRTA) with a reaction rate of 0.06 min^{-1}. For comparison, all three curves are plotted versus temperature. The resulting lines of fitting these data according to eq 2 are plotted in Figure 5. Data obtained under isothermal conditions when plotted according to eq 2 describe a vertical line except when the kinetic model obeyed by the reaction (A2 in this case) is assumed. In this latter case, all data are on a single point. CRTA data allow better discrimination than linear heating rate data, mainly for discriminating among F1 and the different Avrami kinetic models. For all of these models, the linear heating rate yields a perfect straight line, whereas CRTA data only describes a straight line

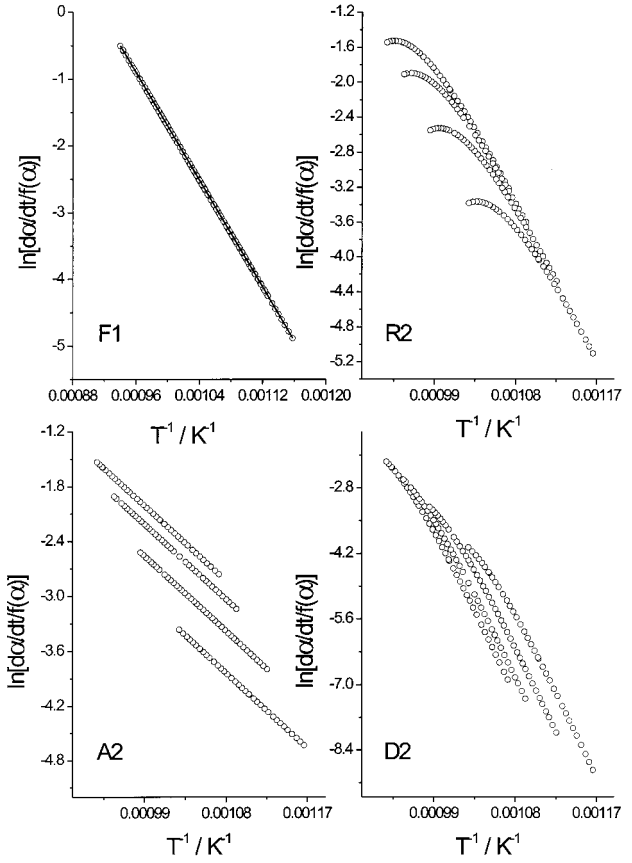

Figure 3. Analyses of the curves included in Figure 2 by means of eq 2 after assuming different kinetic models.

for the correct kinetic model. These results agree with those previously reported[27] that demonstrated that the shapes of CRTA data are more sensitive than the linear heating rate data for discriminating among the kinetic mechanisms. Thus, whereas linear heating rate curves have always a sigmoid shape, the shape of the CRTA curves depend on the kinetic model followed by the reaction: diffusion mechanisms, i.e., D2, D3, and D4, yield sigmoid-shaped curves with an inflection point; nucleation mechanisms, i.e., A1.5, A2, A2.5, A3, and A4, yield curves with a minimum; and *n*-order mechanisms, i.e., F1, R2, and R3, yield curves without minimum or maximum. In summary, these results show that the set of α (or dα/dt) versus time or temperature plots simulated by assuming different heating schedules fit a single straight line only if the kinetic model and the kinetic parameters assumed for calculating the theoretical curves are considered.

4.2. Check of the Method from Experimental Curves. *4.2.1. Crystallization Kinetics of $Ge_{0.3}Sb_{1.4}S_{2.7}$.* Figure 6 shows the DSC results recorded at different heating rates, i.e., 2, 5, 10, and 15 K min^{-1}, for the bulk crystallization of the $Ge_{0.3}Sb_{1.4}S_{2.7}$ glass. The kinetic analysis of these curves was performed by means of eq 2. As a way of example, Figure 7 shows the plots of these data according to eq 2 after assuming four different kinetic models, F1, R2, A2.5, and D2. It is clear from the latter plot that only by assuming an A2.5 kinetic model all of the data are fitted by a single straight line, whose slope and intercept leads respectively to an activation energy of 159 ± 2 KJ mol^{-1} and a Arrhenius preexponential factor equal to (1.1 ± 0.4) 10^{12} min^{-1} with a correlation coefficient r = 0.995. These results are in good agreement with those obtained for the same compound by Malek.[28] To test the calculated parameters, the experimental curves were reconstructed with these

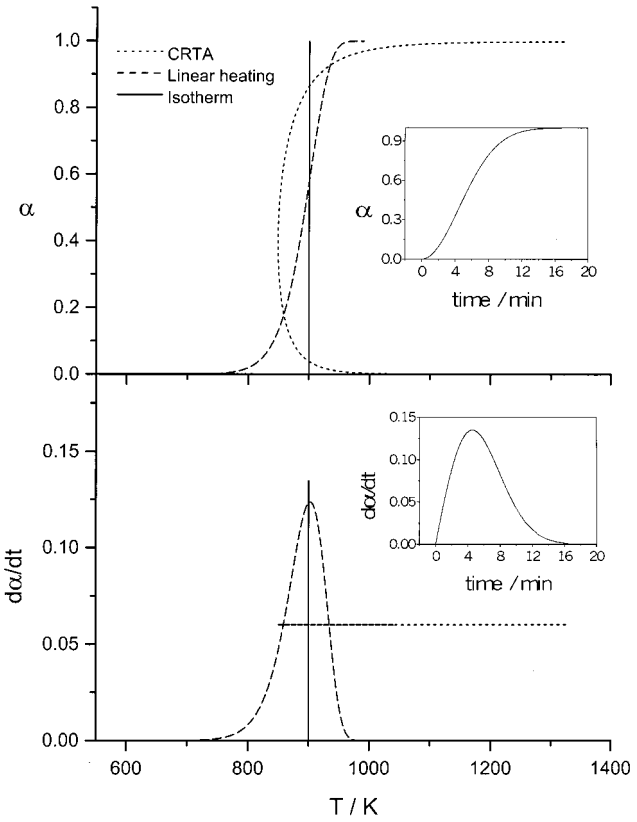

Figure 4. α−*T* plots simulated for an A2 kinetic model by assuming the following kinetic parameters: $A = 10^5$ min^{-1}, $E = 100$ kJ mol^{-1}, and different heating schedules: isothermal (900 °C); linear heating rate ($\beta = 10$ K min^{-1}) and CRTA with a constant reaction rate $C = 0.06$ min^{-1}. The windows show the α (or dα/d*t*) versus time plots calculated for the isothermal at 900 °C.

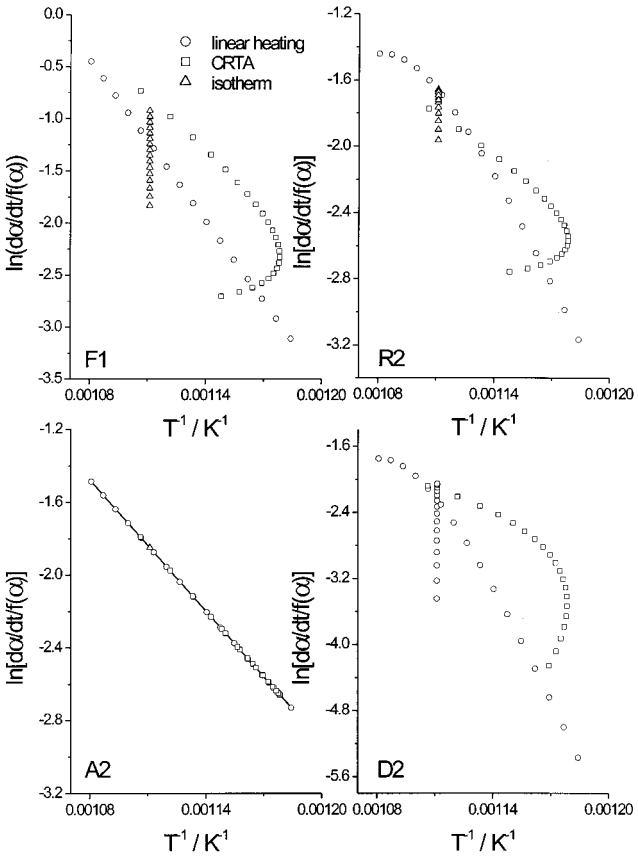

Figure 5. Analyses of the curves included in Figure 4 by means of eq 2 by assuming different kinetic models.

calculated parameters by considering an A2.5 kinetic model. Figure 6 shows the good agreement between calculated and experimental curves for the four experiments. Moreover, the dα/dθ versus α plot calculated from the set of experimental data included in Figure 6 match the master plot corresponding to an Avrami−Erofeev mechanism as shown in Figure 8, which confirms our previous considerations.

The combined analysis of the DSC curves recorded under different heating rates for the crystallization of $Ge_{0.3}Sb_{1.4}S_{2.7}$ allows us to conclude that the reaction rate of this process follows an Avrami−Erofeev mechanism with values of the activation energy and the preexponential factor of Arrhenius that remain constant over all of the crystallization process. This behavior means that the crystallization rate of $Ge_{0.3}Sb_{1.4}S_{2.7}$ is controlled by the growing of previously preexisting nuclei according to the conclusion reached in a previous paper.[28]

4.2.2. Thermal Decomposition Kinetics of Siderite. It has been previously demonstrated with simulated curves that the differential eq 2 can be also applied to the kinetic analysis of data obtained under different heating conditions, i.e., linear heating, isothermal, CRTA, modulated temperature, etc. A set of two curves (Figure 9) has been experimentally obtained for the thermal decomposition of a mineral siderite sample. One of the curves was obtained at a heating rate of 0.52 K min^{-1}, whereas the other curve was obtained under constant decomposition rate of 2.45×10^{-3} min^{-1}. Both curves were analyzed in a combined way by means of eq 2. Figure 10 shows the results obtained by assuming by way of example four different kinetic models (F_1, R_2, A_2, and D_2). These results demonstrate that only when a F1 kinetic model is assumed all of the experimental data are fitted

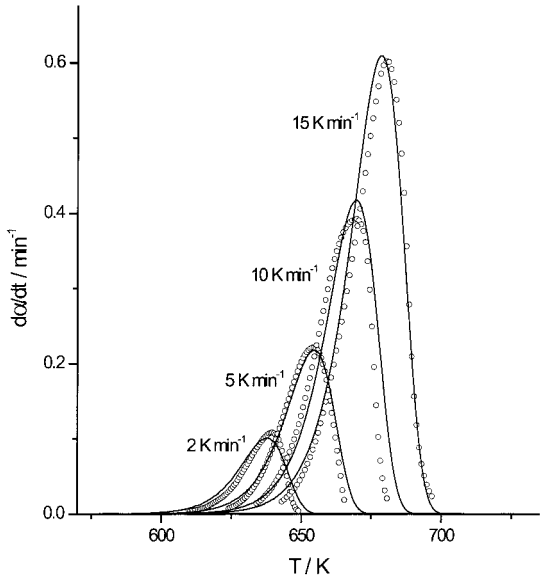

Figure 6. Experimental DSC results (points) recorded at different heating rates ($\beta = 2$, 5, 10, and 15 K min^{-1}) for the bulk crystallization of $Ge_{0.3}Sb_{1.4}S_{2.7}$ glass and reconstructed curves (solid lines) from the kinetic parameters obtained from the combined analysis proposed in this work.

by a single straight line whose slope and intercept lead to an activation energy $E = 185 \pm 1$ KJ mol^{-1} and an Arrenius preexponential factor $A = (5.4 \pm 0.3)\ 10^{10}$ min^{-1} with a correlation coefficient $r = 0.999$. On the other hand, Figure 9 shows that the theoretical curves simulated with these kinetic parameters for a F_1 kinetic model match the experimental curves obtained for the thermal decomposition of siderite. Figure 11

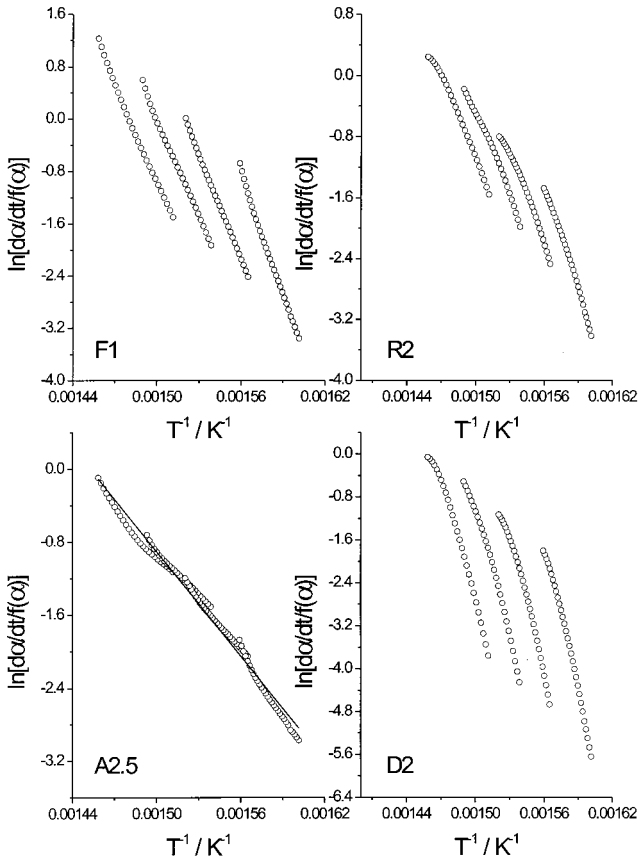

Figure 7. Combined analysis by means of eq 2 of the DSC curves recorded for the crystallization of $Ge_{0.3}Sb_{1.4}S_{2.7}$ glass.

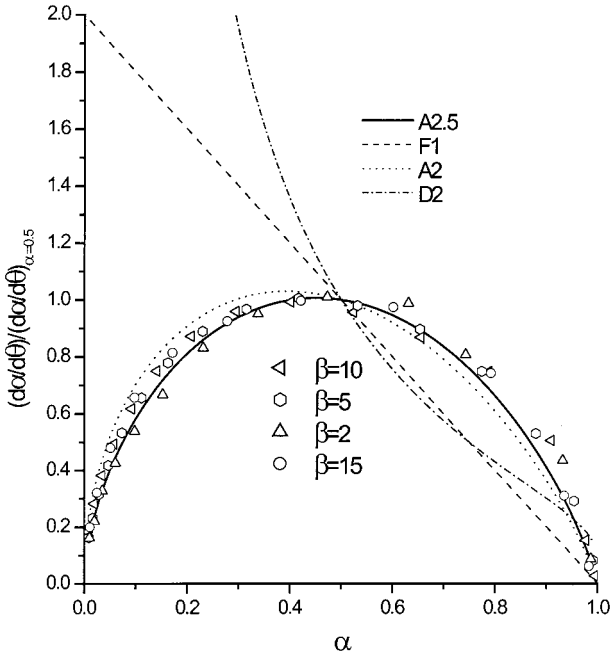

Figure 8. Comparison of the experimental master plots of $(d\alpha/d\theta)/(d\alpha/d\theta)_{0.5}$ against α for the crystallization of $Ge_{0.3}Sb_{1.4}S_{2.7}$ glass with the theoretical master plots.

shows that the $d\alpha/d\theta$ versus α plot calculated from the set of experimental data included in Figure 9 match the master plot corresponding to a F_1 kinetic model, which confirms our previous conclusion.

The reconstruction of the experimental curves with simulated curves obtained with the calculated kinetic parameter is a useful

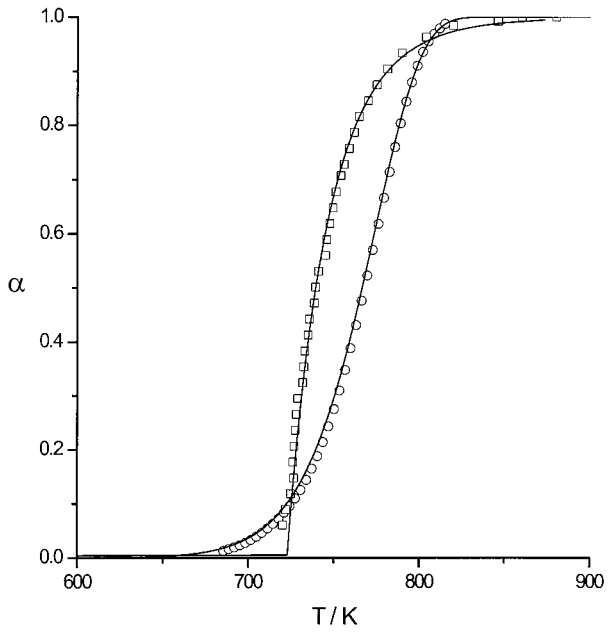

Figure 9. Thermal decomposition of a siderite mineral sample. (○) Experimental TG curve recorded under a linear heating rate of 0.52 K min^{-1}. (□) Experimental CRTA curve under a constant reaction rate of 2.45 10^{-3} min^{-1}. Simulated curves constructed by assuming the kinetic parameters obtained from the analysis of the experimental curves by means of eq 2 (solid lines).

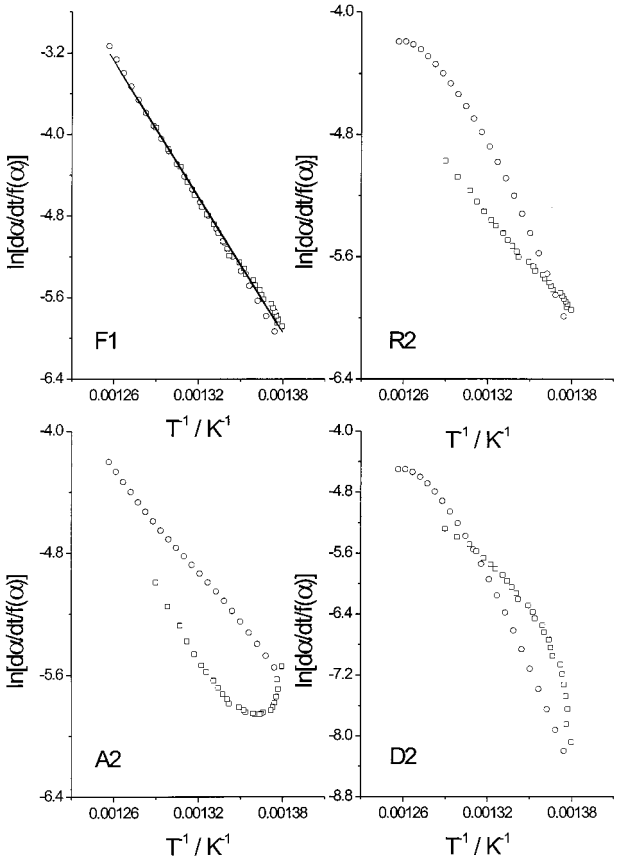

Figure 10. Combined analysis by means of eq 2 of the TG and CRTA curves obtained for the thermal decomposition of siderite.

method for checking the results obtained by this kinetic analysis. Curves obtained under different experimental conditions are expected to be affected by different heat and mass transfer phenomena. The fact that all of the curves are reconstructed

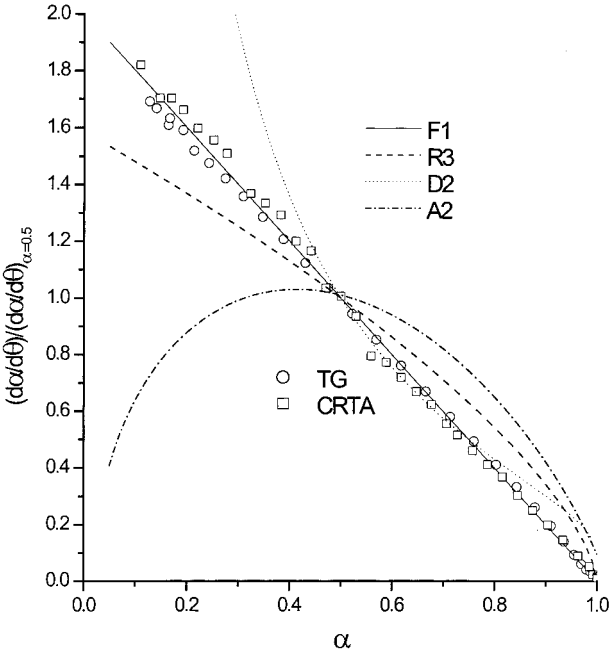

Figure 11. Comparison of the experimental master plots of $(d\alpha/d\theta)/(d\alpha/d\theta)_{0.5}$ against α for the thermal decomposition of siderite with the theoretical master plots.

with the same kinetic parameters seem to indicate that these mass and heat transfer phenomena are minimized. An alternative method for checking the results is by means of the universal master plot previously proposed by using the concept of generalized time.[17] These master plots can be used for data obtained under any heating schedule.

5. Conclusions

The use of the general kinetic equation in the logarithmic form (eq 2) can be used to fit experimental data obtained under any conditions because no assumptions are made on the heating schedule used. Thus, data obtained under different experimental conditions such as isothermal, linear heating, modulated temperature, sample controlled, etc. can be analyzed in a combined way. An additional advantage of this method is that data can be analyzed even when the experiment has not been performed under the optimum experimental conditions. For example, if in a linear heating rate experiment there are deviations in the temperature−time line, or in CRTA if the reaction rate is not maintained constant, or in isothermal experiment if there are fluctuations in the temperature, or if the steady stage is reached after that, the reaction has already started. The only assumption is that the $T - \alpha - d\alpha/dt$ data sets have been properly measured.

A set of curves obtained under linear heating rate conditions at different heating rates have been analyzed by eq 2. It has been shown that, although a curve obtained under a linear heating rate condition can be fitted by more than a single kinetic equation, curves obtained under different linear heating rate conditions are fitted only by a single mechanism. This procedure has been tested experimentally with a set of curves obtained under linear heating rate conditions for the crystallization of $Ge_{0.3}Sb_{1.4}S_{2.7}$ glass. A A2.5 kinetic model and an activation energy of 159 ± 2 KJ mol^{-1} were obtained. The resulting kinetic parameters allowed one to simulate kinetic curves that agreed very well with the experimental data. In addition, simulated curves obtained assuming linear heating, isothermal, and constant reaction rate conditions were analyzed in a combined way by eq 2 yielding a unique result that fitted all data. Two experimental curves for the thermal decomposition of a natural siderite sample under linear heating and CRTA conditions were analyzed by this method, yielding an F1 kinetic model and an activation energy of 185 ± 1 KJ mol^{-1}, and these kinetic parameters allowed the reconstruction of both curves.

References and Notes

(1) Rouquerol, J. *Thermochim. Acta* **1997**, *300*, 247.
(2) Pérez-Maqueda, L. A.; Subrt, J.; Criado, J. M.; Real, C. *Catal. Lett.* **1999**, *60*, 151.
(3) Pérez-Maqueda, L. A.; Criado, J. M.; Real, C.; Subrt, J.; Bohácek, J. *J. Mater. Chem.* **1999**, *8*, 1839.
(4) Chopra, G. S.; Real, C.; Alcalá, M. D.; Pérez-Maqueda, L. A.; Subrt, J.; Criado, J. M. *Chem. Mater.* **1999**, *11*, 1128.
(5) Sorensen, O. T. *J. Therm. Anal.* **1992**, *38*, 213.
(6) Blaine, R. L.; Hahn, B. K. *J. Therm. Anal. Calorim.* **1998**, *54*, 695.
(7) Ozawa, T. *Thermochim Acta* **2000**, *356*, 173.
(8) Galwey, A. K.; Brown, M. E. In *Handbook of Thermal Analysis and Calorimetry*; Brown, M. E., Ed.; Elservier Science: Amsterdam, 1998; Vol. 1 Principles and Practise, p 147.
(9) Sharp, J. H.; Brindley, G. W.; Archar, B. N. N. *J. Am. Ceram. Soc.* **1966**, *49*, 379.
(10) Brown, M. E.; Dolimore, D.; Galwey, A. K. *Thermochim. Acta* **1977**, *21*, 103.
(11) Brown, M. E.; Dolimore, D.; Galwey, A. K. *J. Chem. Soc., Faraday Trans.* **1974**, *70*, 1316.
(12) Freeman, E. S.; Carrol, B. *J. Phys. Chem.* **1958**, *62*, 394.
(13) Friedman, H. L. *J. Polym. Sci.* **1965**, *66*, 183.
(14) Ozawa, T. *Bull. Chem. Soc. Jpn.* **1965**, *38*, 1881.
(15) Vyazovkin, S.; Dollimore, D. *J. Chem. Inform. Comput. Sci.* **1996**, *36*, 42.
(16) Kissinger, H. E. *Anal. Chem.* **1957**, *29*, 1702.
(17) Gotor, F. J.; Criado, J. M.; Malek, J.; Koga, N. *J. Phys. Chem. A* **2000**, *104*, 10777.
(18) Criado, J. M.; Morales, J. *Thermochim. Acta* **1977**, *19*, 305.
(19) Criado, J. M.; Ortega, A. *J. Therm. Anal.* **1984**, *29*.
(20) Ozawa, T. *J. Therm. Anal. Calorim.* **2000**, *59*, 375.
(21) Ozawa, T. *J. Therm. Anal. Calorim.* **2001**, *64*, 109.
(22) Ozawa, T. *Thermochim. Acta* **1986**, *100*, 109.
(23) Ozawa, T. *J. Therm. Anal.* **1970**, *2*, 301.
(24) Chai, L.; Navrrotsky, A. *Geochim. Cosmichim. Acta* **1996**, *60*, 4377.
(25) Rouquerol, J.; Bordere, S.; Rouquerol, F. *Thermochim. Acta* **1992**, *203*, 193.
(26) *Mathcad_8_professional*; MathSoft, Inc: Cambridge, MA, 1998.
(27) Criado, J. M.; Ortega, A.; Gotor, F. *Thermochim. Acta* **1990**, *157*, 171.
(28) Malek, J. *Thermochim. Acta* **2000**, *355*, 239.